METEOROLOGICAL APPLICATIONS
Meteorol. Appl. (2012)
Published online in Wiley Online Library
(wileyonlinelibrary.com) DOI: 10.1002/met.1291

Characterizing North Atlantic weather patterns for climate-optimal aircraft routing

Emma A. Irvine,[a]* Brian J. Hoskins,[a,b] Keith P. Shine,[a] Robert W. Lunnon[a] and Christine Froemming[c]
[a] *Department of Meteorology, University of Reading, UK*
[b] *Grantham Institute for Climate Change, Imperial College London, UK*
[c] *Institut für Physik der Atmosphäre, Deutsches Zentrum für Luft- und Raumfahrt, Oberpfaffenhofen, Germany*

ABSTRACT: Daily weather patterns over the North Atlantic are classified into relevant types: typical weather patterns that may characterize the range of climate impacts from aviation in this region, for both summer and winter. The motivation is to provide a set of weather types to facilitate an investigation of climate-optimal aircraft routing of trans-Atlantic flights (minimizing the climate impact on a flight-by-flight basis). Using the New York to London route as an example, the time-optimal route times are shown to vary by over 60 min, to take advantage of strong tailwinds or avoid headwinds, and for eastbound routes latitude correlates well with the latitude of the jet stream. The weather patterns are classified by their similarity to the North Atlantic Oscillation and East Atlantic teleconnection patterns. For winter, five types are defined; in summer, when there is less variation in jet latitude, only three types are defined. The types can be characterized by the jet strength and position, and therefore the location of the time-optimal routes varies by type. Simple proxies for the climate impact of carbon dioxide, ozone, water vapour and contrails are defined, which depend on parameters such as the route time, latitude and season, the time spent flying in the stratosphere, and the distance over which the air is supersaturated with respect to ice. These proxies are then shown to vary between weather types and between eastbound and westbound routes. Copyright © 2012 Royal Meteorological Society

KEY WORDS aviation; teleconnections

Received 1 April 2011; Revised 14 September 2011; Accepted 14 November 2011

1. Introduction

Aircraft emissions contribute to anthropogenic climate change through emissions of carbon dioxide (CO_2), water vapour (H_2O) and oxides of nitrogen, NO_x, (which influence ozone (O_3) and methane concentrations), as well as by forming contrails and possibly influencing natural cirrus. The contribution of aviation to the global anthropogenic CO_2 emissions over the last 50 years has been calculated to have increased to 2.5% (Lee *et al*., 2009). The non-CO_2 climate effects due to aviation are much more uncertain, but it has been estimated that including these additional impacts means that aircraft emissions contribute about 4.9% when including the uncertain effects of contrail cirrus (with a range of 2–14%) of the present-day total anthropogenic radiative forcing (Lee *et al*., 2009, 2010). Industry predictions of passenger transport give a continued growth of around 5% *per* year (Lee *et al*., 2009), against a background of continued political pressure to reduce aviation and other anthropogenic emissions.

There are two approaches to reducing emissions from aviation: operational and technological. The latter includes development of lighter airframes, more efficient engines and cleaner fuels to replace the existing technologies. Operational changes have the advantage of using existing technology and, therefore, these methods are quicker and cheaper to develop and implement. Operational changes include improved air traffic management procedures by air-traffic control (ATC), such as reduced time holding and more direct flights. Such measures are already being introduced by the UK National Air Traffic Services (NATS), leading to CO_2 savings of 50 000 tonnes in 2010 (NATS, 2010). Another measure is using an environmentally-friendly flight profile, where an aircraft uses a continuous descent approach (descent at a steady rate instead of a stepped descent): these are already used at many UK airports, and can lead to small CO_2 savings (a saving of 1% fuel burn *per* trip) even when implemented from relatively low altitudes (Ren *et al*., 2010). Climate-optimized routing is another possible operational measure, where flight trajectories are optimized such that the resulting aircraft emissions have the minimum climate impact, rather than minimizing the time, fuel or operating costs. This approach takes advantage of the fact that the climate impact of aircraft emissions depends on the latitude and altitude at which the emissions take place and on the weather systems encountered on the route, as well as the time of year, and possibly even the time of day.

The work presented here is part of the European Union Framework 7 Collaborative Project REACT4C (Reducing Emissions from Aviation by Changing Trajectories for the Benefit of Climate) which aims to examine the feasibility of climate-optimized routing, for trans-Atlantic flights between Europe and North America. Here, and in the REACT4C project, many climate impacts from aviation (CO_2, H_2O, NO_x and contrails) are considered. The initial focus is on the North Atlantic Flight Corridor (NAFC), which is approximately the area 30–75°N, 10–60°W, between 200 and 300 hPa. In this region there are approximately 300 flights *per* day in each direction (eastbound or westbound), and this relatively small section

*Correspondence to: E. A. Irvine, Department of Meteorology, University of Reading, Earley Gate Reading, RG6 6BB, UK.
E-mail: e.a.irvine@reading.ac.uk

of global airspace contributes 6.5% of total aviation emissions, of which 97% are above 7 km (Wilkerson *et al.*, 2010).

A full assessment of the feasibility of climate optimal route planning is a complex task. First, as noted, there are large uncertainties in estimating the climate impact of non-CO_2 emissions, in particular those relating to aviation-induced contrails and the modification of clouds due to aerosols resulting from aviation emissions – this area has been recently reviewed by Lee *et al.* (2010). Second, these climate impacts depend strongly on highly variable weather conditions (such as the height of the tropopause and the presence of ice supersaturated layers in the upper troposphere): a full evaluation would require models which include, in addition to the meteorology, detailed microphysical and photochemical representations, which makes determining the climate impact of aircraft emissions computationally expensive. Third, it is not straightforward to compare the climate impact of different aviation impacts, primarily because of the different timescales involved in the different processes. For example, because of the impact of additional CO_2 emitted by burning of fossil fuels on the carbon budget, CO_2 concentrations are believed to remain elevated for centuries or longer, following an emission; by contrast, contrails persist for only minutes to hours. There is no unique way of placing these climate impacts on a common scale to enable an assessment of whether, for example, it is desirable from a climate point of view to avoid contrail formation at the cost of emitting more CO_2. A number of 'climate metrics' aimed at enabling such a comparison have been proposed. However, the choice of which climate metric to adopt in practice depends on the aims of climate optimization (different metrics would be chosen if the aim was to avoid short-term rather than long-term climate change), see the recent review by Fuglestvedt *et al.* (2010). Finally, even if climate-optimal routes could be identified, air traffic control considerations may place heavy constraints on whether they are feasible in practice, especially in busy air space.

This study presents one of the necessary first steps in the process of evaluating climate-optimal routing. Its aim is to classify daily weather patterns over the North Atlantic region into relevant weather types, typical weather patterns that may characterize the range of climate impacts of aviation in the region, for both winter and summer and demonstrate that the climate impact associated with flying through these different meteorological conditions is indeed likely to differ by type. The motivation for synoptic typing is to facilitate the climate-optimization of trans-Atlantic flights by other partners within REACT4C, as due to computational costs it is not feasible to calculate the climate-optimized route for each daily weather pattern. Additionally, the weather types that are defined are required to occur sufficiently frequently that it is worth assessing the climate-optimized routing. For each type, the pattern of upper-level winds and, therefore, the optimal, route, should differ. Typically, studies which seek to identify weather regimes over the Atlantic focus on the surface to mid-levels (see e.g. Vautard, 1990; Michelangeli *et al.*, 1995, and references therein). Woollings *et al.* (2010) analysed preferred positions of the maxima in the North Atlantic eddy-driven lower tropospheric westerly wind: the atmospheric patterns associated with these positions relate to three of the regimes identified by Vautard (1990) and Michelangeli *et al.* (1995) (the fourth is a Greenland blocking). Whilst the eddy-driven jet is a barotropic feature that is also present at high altitudes where aircraft fly, there can in addition be upper tropospheric features that would be missed by the Woollings *et al.* (2010) methodology, particularly those associated with the subtropical jet. In identifying weather types that will result in different aircraft routings it is therefore necessary to use relevant higher-level fields for the synoptic typing.

In order to assess whether the climate impact of aircraft emissions differs by weather type, simple proxies for the individual climate impacts (of CO_2, NO_x) are identified. The proxies are simplified by making assumptions about the behaviour of the aircraft during cruise, so that they can be calculated without the use of a fuel burn model, ensuring that the results are independent of aircraft or engine type. It is assumed that the aircraft minimizes the air-distance flown at a constant flight level, which is equivalent to minimizing the fuel burn, and that the rate of fuel burn is constant. In reality the rate of fuel burn will be higher at the beginning of cruise when the aircraft may be 30% heavier, due to the weight of the fuel. During flight the aircraft burns fuel and becomes lighter: in order to maximize the lift to drag ratio the aircraft must either ascend to a higher flight level (thus maintaining airspeed) or slow down (maintaining flight level). Due to the nature of the airspace, on trans-Atlantic flights the flight level and cruise speed of an aircraft may be somewhat constrained by air traffic control: therefore these assumptions are not without basis. Despite the simplicity of the proxies, it will be shown that they work well in identifying differences in the expected climate impact resulting from flights through different weather situations.

The paper is organized as follows. The meteorological and time optimal route data are described in Section 2. An analysis of the optimal route data is presented in Section 3. First, the relationship between the time-optimum route latitude and jet stream latitude is explored for both eastbound and westbound flights. Next, indicative proxies for the different climate impacts of aircraft emissions are identified, to allow an assessment of whether the CO_2 and non-CO_2 climate impacts are likely to differ between the different weather types. The methodology for identifying the weather types is described in Section 4. The defined weather types are presented separately for winter and summer in Section 5, and the indicative climate proxies are then applied to each type (separately for eastbound and westbound flights) in Section 6. Conclusions are presented in Section 7.

2. Data

2.1. Meteorological data

The weather patterns are analysed using the European Centre for Medium-Range Weather Forecasts (ECMWF) Re-Analysis Interim (ERA-Interim) dataset (Dee *et al.*, 2011). This covers a period of 21 years from 1989 to 2010 at 0.7° horizontal resolution. For this study the period June 1989 to February 2010 was used to provide 21 complete winter and summer seasons. An advantage of using ERA-Interim data is that the ECMWF model cloud scheme now explicitly allows for ice-supersaturation (Tompkins *et al.*, 2007), which is a required condition for contrail formation. The locations of regions of ice-supersaturation in the ECMWF forecasts have been shown to verify well against radiosonde humidity measurements over England (Rädel and Shine, 2010).

The latitude of the westerly wind maximum at 250 hPa (flight level) is calculated from ERA-Interim as in Woollings *et al.* (2010). The zonal wind is averaged over the North Atlantic sector (0–60 °W), and then the latitude of the maximum is searched for between 30 and 75°N. The latitude of

this westerly wind maximum is taken as the jet latitude (note that this method does not have a wind speed criterion).

2.2. Time-optimal aircraft routes

Time-optimized route data (referred to as optimal routes) were provided by the Met Office, generated using their optimal route software (Lunnon, 1992) run on the Unified Model (MetUM) wind forecasts. For the period of interest, the horizontal grid-spacing of the MetUM forecasts was 40 km prior to February 2010 and 25 km thereafter. These data provide the quickest route between two specified airports, assuming a constant true airspeed and a constant flight level. For this study a constant true airspeed of 250 m s^{-1} (560 mph, 900 km h^{-1}) is used, representative of the cruise speed of a modern aircraft, and a constant flight level of 250 hPa (about 10 km or flight level (FL) 340), thus neglecting take-off and landing or any in-flight changes in cruise altitude. Aircraft flight levels are specified as a pressure altitude in hundreds of feet (FL340 is 34 000 ft) where the pressure altitude is calculated using the International Civil Aviation Organization (ICAO) standard atmosphere (which assumes a dry atmosphere with a surface pressure of 1013.25 hPa, surface temperature of 15 °C and lapse rate of 1.8 °C *per* 1000 ft, which is close to 6 °C km^{-1}). The flight level chosen for this study is in the middle of the permitted cruise altitudes, which correspond to 200–300 hPa, over the North Atlantic flight corridor. If the time optimal routes are instead calculated using the 200 hPa or 300 hPa winds, their location is within 1° of the route at 250 hPa: therefore vertical variations in the horizontal wind are neglected when defining the optimal routes. The justification for the use of a constant cruise speed and altitude is that aircraft flying on the ATC-defined North Atlantic tracks normally maintain a constant cruise speed and altitude for the duration of the crossing due to the limited radar coverage over the ocean (though a limited number of altitude changes may be allowed).

The time-optimal route between London Heathrow airport (EGLL) and New York JFK airport (KJFK) is used, and this is taken to be representative of the location of trans-Atlantic air traffic. To check this assumption, the location of the North Atlantic tracks, which are a good indication of the location of trans-Atlantic air traffic on any given day, was examined. The North Atlantic tracks consist of five to eight parallel paths across the Atlantic, laterally separated by a minimum of 1° latitude, defined over oceanic airspace (between approximately 10 and 60 °W). They are defined twice-daily by air-traffic control, guided by the flight plans filed by airlines for that day: an eastbound set for night-time flights to Europe, and a westbound set for daytime flights to the USA. Approximately 50% of trans-Atlantic flights use the North Atlantic tracks; the rest of the air traffic fly alternative routes, which may use part of the North Atlantic tracks (ICAO, 2008). A comparison was undertaken of the location of the EGLL-KJFK time-optimal routes (provided by the Met Office) and North Atlantic tracks (supplied by the UK National Air Traffic Services (NATS)), for summer 2009 and winter 2009–2010. For this period, the New York to London time-optimal route lay within the ATC-defined North Atlantic tracks on 74–93% of days: this, therefore, confirms that the New York to London time-optimal route is appropriate to use to represent the location of air traffic over the North Atlantic. For simplification, when using the time-optimal routes, it is assumed that eastbound flights would depart North America at 0000 UTC, westbound flights would depart Europe at 1200 UTC and that they all fly through a weather situation that does not change during their flight (note that the predicted time evolution of the wind field is taken into account in the computation of the time-optimal routes).

Optimum route data for the winters (December, January and February) of 2004–2005, 2008–2009 and 2009–2010 are analysed. These winters were chosen because of their different large-scale North Atlantic atmospheric circulations and jet latitudes (Figure 1). The 2009–2010 winter mean jet latitude was 39°N, one standard deviation further south than the 1989–2010 ERA-Interim winter mean of 49°N (Figure 1(a)). This was related to the unusually large negative North Atlantic oscillation (NAO) index (Figure 1(c)). The winter of 2004–2005 also had a highly skewed distribution of jet latitude, this time with the jet stream further North than average, related to a positive NAO and negative East Atlantic (EA) index (see Section 4 for an extended discussion of the NAO and EA indices). In contrast, in 2008–2009 the NAO and EA were weak and the jet latitude was quite normally distributed around the climatological average. In summer (June, July and August) there is less variation in jet latitude and the jet stream is located further north than in winter (not shown); therefore optimum route data for only one summer, 2009, were used.

3. Analysis of optimum route data

The relationship between the location of the maximum westerly winds and the time-optimum route is examined. The time-optimum route data are also analysed to see the variation in route time and distance that arises due to the variability in the strength and location of flight-level winds.

3.1. Route latitude

The location of the time-optimized routes varies daily depending on the pattern of winds over the North Atlantic. The latitude of the optimum route is related to the position of the upper-level jet stream, identified following Woollings *et al*. (2010) (Figure 2). For eastbound routes (Figure 2(a)) there is good correspondence between the optimal route latitude at 40 °W and the jet stream latitude, except when the jet stream moves south of 35 °N and the quickest route is to fly close to a great circle north of the jet stream. Excluding these most southerly latitudes, the linear correlation between the jet stream latitudes (from 35 to 70 °N) and route latitude is 0.73. In summer the jet stream is on average further north and the subtropical jet is absent: therefore, there is also good correspondence between the route latitude and jet stream latitude (not shown). For westbound routes (Figure 2(b)) the optimum routes are located further from the jet stream, in order to minimize headwinds. In winters when the jet stream is located further south, for example 2009–2010, the westbound optimum route is most often north of the jet stream, and vice versa for a more northerly jet stream in 2004–2005. In the winter of 2008–2009 there was a large spread in jet latitude. The resulting westbound routes lie equally to the north or south of the jet stream and there is a small spread in eastbound route latitude, both indicative of a weaker jet stream.

3.2. Climate characteristics

The climate impacts of aviation that are considered here are the effects of CO_2, NO_x-induced O_3, water vapour and contrails. The radiative forcings for many of the non-CO_2 impacts are uncertain and their calculation is computationally expensive:

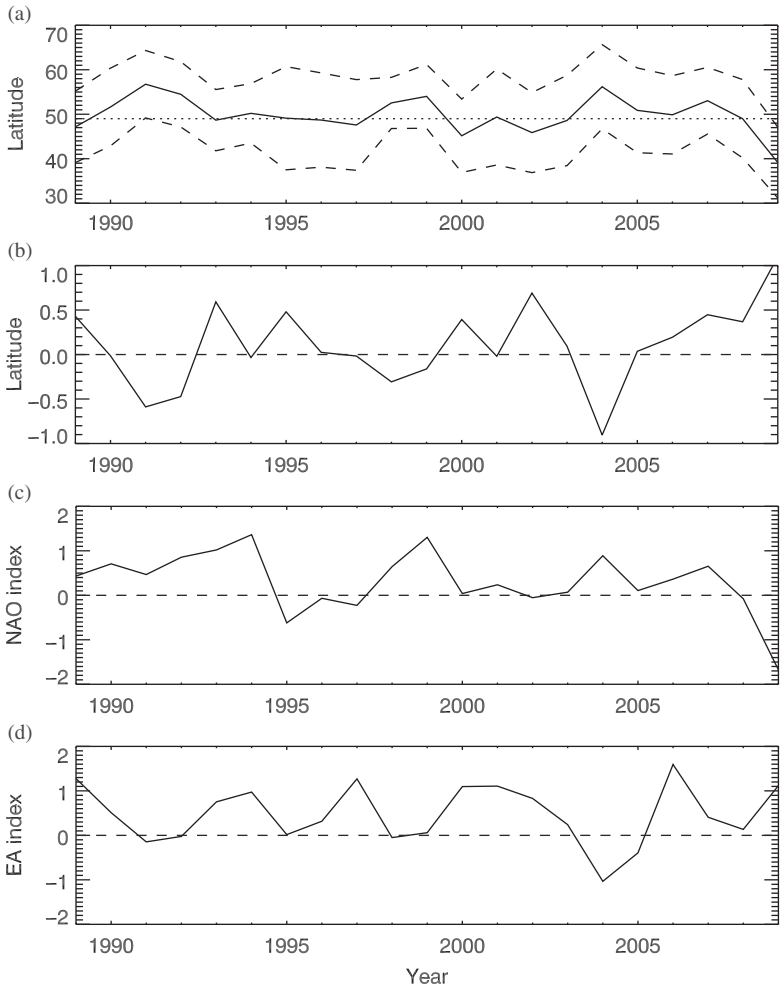

Figure 1. (a) Time series of the winter (DJF) mean jet latitude in ERA-Interim (solid line) and the intra-seasonal standard deviation (dashed lines). The 1989–2009 winter mean jet latitude is overlaid on (a) (dotted line). (b) The time-series of the intra-seasonal skewness of the winter jet latitude in ERA-Interim. Time series of (c) NAO index and (d) EA index for the same period. The year on the axes corresponds to the December of each winter.

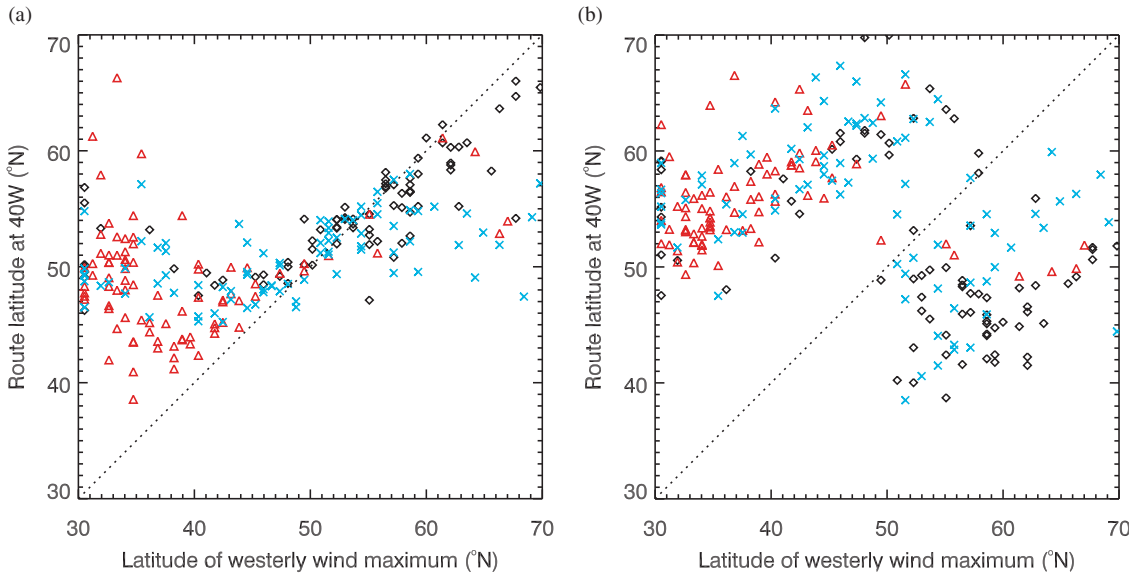

Figure 2. Latitude at which the optimum route crosses 40 °W against the latitude of the zonally averaged westerly wind maximum at 250 hPa for (a) eastbound and (b) westbound routes. Data are plotted for three winters: 2004–2005 (diamonds), 2008–2009 (crosses) and 2009–2010 (triangles). If the optimum route at 40 °W was always at the same latitude as the westerly wind maximum then the points would lie along the 1 : 1 line. This figure is available in colour online at wileyonlinelibrary.com/journal/met

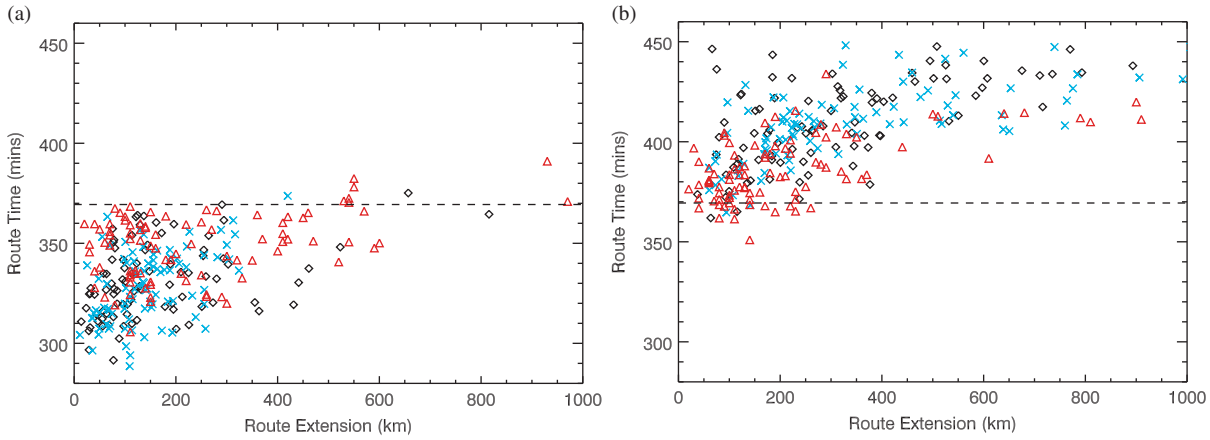

Figure 3. Time taken to fly the optimum route *versus* route extension (route distance minus great circle distance) for (a) eastbound and (b) westbound flights between New York JFK airport and London Heathrow airport. Data are plotted for three winters: 2004–2005 (diamonds), 2008–2009 (crosses) and 2009–2010 (triangles). The time taken to fly the great circle distance in still air is shown by the dashed line. This figure is available in colour online at wileyonlinelibrary.com/journal/met

this is an aim elsewhere in the REACT4C project. However, it is useful to introduce simple proxies of the climate effect of the aircraft emissions here, to give an indication of the possible variation in climate impact which would result from flying a time-optimal route through different weather situations in the North Atlantic, and to help motivate the more detailed calculations.

The climate impact of CO_2 is proportional to the total amount of CO_2 released during the flight and, as CO_2 is a long-lived (and hence, relatively well-mixed) gas, the impact is independent of the emission location, and the rate of fuel burn is irrelevant. For constant flight level and fuel burn, the climate impact of CO_2 is related to the air-distance travelled. This is the product of the route time (calculated taking into account the winds at flight level) and true airspeed, which, as stated in Section 2.2, is assumed to be constant. Therefore, the route time is used as a simple proxy for the climate impact of CO_2. The climate impact is therefore greater for longer flights, which require more fuel and therefore produce greater amounts of CO_2. Figure 3 shows the optimum route time as a function of the route extension (the difference between the optimal route distance and the great circle distance) for winter. Note that if there was no wind, an aircraft would fly a great circle route (a route extension of 0 km): for a flight between London and New York the great circle distance is 5541 km, and for a constant true airspeed of 250 m s^{-1} the corresponding time of flight in still air is 369.4 min (dashed line in Figure 3). Eastbound routes (Figure 3(a)) are generally shorter and quicker than westbound routes (Figure 3(b)) which have to avoid strong headwinds. The range of route times is approximately 60 min for eastbound flights, and 80 min for westbound flights, and eastbound routes are almost always shorter than westbound routes. For instance, the westbound routes in winter 2009–2010 are quickest as the jet stream was generally further south, associated with the strong negative NAO signal.

At a constant cruise altitude of 250 hPa the climate impact of NO_x-induced O_3 is dependent on emission latitude: the impact is largest at the equator and decreases towards the poles (Grewe and Stenke, 2008; Fichter, 2009), although the impact of any individual flight will depend somewhat on the direction in which the emitted NO_x is advected, vertical transport and possible subsequent washout *via* HNO_3. The simplified climate impact proxy adopted here (defined in Section 6.1) is therefore a function of the route latitude. The optimum route latitude at 40 °W ranges from 40 to 70 °N and shows a large range within a single season. In summer this range is smaller, as the jet location is on average located further north, in a favourable location for eastbound flights. The summer flights would lead to greater ozone production than the winter flights, as the photochemical O_3 production from NO_x is more efficient in summer; because of the lack of sunlight, there is only a small O_3 penalty for flying at high latitudes in winter. Note that the climate effect of NO_x-induced ozone increases is significantly offset by an accompanying longer-lived decrease in methane (plus a methane-induced decrease in ozone), so the net climate impact of NO_x changes is less easy to compute (e.g. Lee *et al*., 2010; Fuglestvedt *et al*., 2010).

The climate impact of water vapour emissions, and to an extent, NO_x emissions, is increased if the emissions are made directly into the stratosphere where they have a longer lifetime (e.g. Gettelman, 1998; Forster *et al*., 2003): therefore the total route time that the aircraft would be in the stratosphere is considered a simplified climate impact proxy. To determine whether an aircraft would be in the stratosphere, following Wilcox *et al*. (2011), a dynamic tropopause where the potential vorticity is 2 PVU is defined. Figure 4 shows transects along the time optimum route for two winter cases that would likely result in a different climate impact from water vapour emissions. In Figure 4(a) at 250 hPa the route is entirely in the stratosphere. In Figure 4(b) at 250 hPa the route is mostly in the troposphere, and so the climate impact due to water vapour emissions would be smaller than for the route in Figure 4(a). The mean route time in the stratosphere is 0.6 of the total route time for the optimum routes in winter, and 0.42 and 0.55 for, respectively, the eastbound and westbound optimum routes in summer.

Lastly, the climate impact from contrails formed as a result of mixing hot moist exhaust air with cooler ambient air is considered, using the total distance over which an aircraft would produce a persistent contrail, defined by the Schmidt-Appleman criterion (Schumann, 1996) to be regions where the air is supersaturated with respect to ice and the ambient air temperature is below 233 K as a proxy. As is the case for the examples shown in Figure 4, the regions of supersaturation are generally small. By virtue of spending more time in the troposphere, the route in Figure 4(b) is more likely to

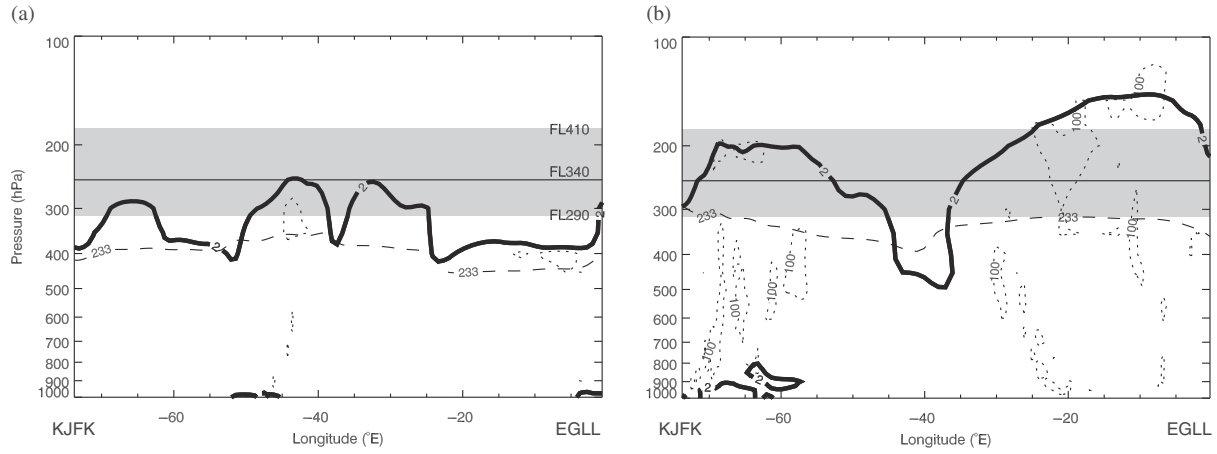

Figure 4. Transects along the eastbound optimum route from New York JFK airport (KJFK) to London Heathrow airport (EGLL) for (a) 18 February 2010 and (b) 26 January 2010, both at 0000 UTC. The optimum routes assume a constant cruise altitude of 250 hPa (thin black line); the range of permitted cruise altitudes in the North Atlantic flight corridor is 315–180 hPa (grey shading). Along the route the height of the dynamic tropopause (thick black line), 233 K isotherm (dashed line) and ice-supersaturated regions (dotted lines) are shown. Persistent contrails could form at altitudes above the 233 K isotherm and within the ice-supersaturated regions.

produce persistent contrails. Note that, perhaps surprisingly, in Figure 4(b) there is a small region of supersaturation at 10 °E, some of which appears to be in the stratosphere (at least, using the 2 PVU definition). In fact, for the winter optimal route data, on 12% of days the routes would produce some stratospheric contrails. Using commercial aircraft measurements of relative humidity Gierens *et al*. (1999) found that 2% of the data points in the stratosphere showed ice supersaturation. This result is corroborated by microwave limb sounder measurements of humidity (Spichtinger *et al*., 2003).

Note that the climate proxies we derive are to give a first indication of how each individual climate effect varies between the derived weather types, no attempt is made here to compare between different climate effects and discuss climate-optimal routes, which is a wider aim of the REACT4C project.

4. Methodology

To split the weather patterns into types, the similarity of the daily geopotential height anomaly field to the NAO and EA teleconnection patterns described below (Figure 5) is considered: both are leading modes of variability in the North Atlantic in both winter and summer. The patterns are constructed by regressing monthly-mean geopotential height anomalies at 250 hPa (Z250) onto the monthly-mean NAO and EA indices (the indices are available at http://www.cpc.ncep.noaa.gov/data/teledoc/telecontents.shtml). The positive phase of the wintertime NAO (Figure 5(a); Barnston and Livezey, 1987) consists of a north–south oriented dipole of a negative height anomaly over Greenland and positive height anomaly to its south over the North Atlantic, and is associated with a northward shift in the jet stream. In the negative phase, the signs of the height anomalies are reversed, resulting in a southward shift in the jet stream. The EA pattern (Figure 5(b)) resembles a south-eastward shifted NAO pattern, so that the dipole axis has a southwest-northeast tilt. In summer the patterns are weaker (Figure 5(c) and (d)), and the NAO dipole is shifted. As the jet stream latitude can be quite well described by the NAO and EA indices (Woollings *et al*., 2010) this methodology should yield types with different jet positions: from Figure 2 it is clear that this will result in different optimal routes.

To determine the types, the daily anomalies of Z250 data are calculated, first removing the seasonal cycle by Fourier filtering. By using daily data, all days from the 21 complete summer and winter seasons in the ERA-Interim dataset are classified. These daily anomalies are then projected onto each of the NAO and EA patterns, by calculating the inner product of the daily Z250 anomaly with the NAO or EA pattern, and the projection coefficients plotted (Figure 6). By normalizing the inner-product calculation, the projection coefficients are constrained to be between 1 and −1, where a coefficient of 1 indicates that the anomaly field has the same structure as the teleconnection pattern, −1 that the anomaly field has the same structure of opposite sign, and 0 that the anomaly field is orthogonal to it. To obtain the weather types, the projection coefficients are split according to a subjectively-determined threshold value, chosen to identify only a small number of frequently occurring types. The thresholds used are 0.4 for winter, 0.3 for summer (Figure 6). The full Z250 and 250 hPa wind speed (v250) fields for days belonging to each type are composited. Reasonable changes (0.1) in the threshold used results in similar patterns.

5. Meteorological types

5.1. Winter

Five distinct weather types (referred to here as types W1 to W5) are defined for winter. For each type, composites of Z250 and v250 are made, using all days from the ERA-Interim dataset that belong to that type. The minimum number of days making up the composite for any type is 320 (Figure 7). Figure 7 shows Z250 and v250 for each type, together with the optimum routes corresponding to days that are in that weather type, separately for eastbound and westbound routes: the great circle route for New York to London is also shown. The composites indicate that the five types can be characterized by the strength and location of the jet at 250 hPa, and Table 1 summarizes each type, in terms of jet characteristic and the frequency *per* season.

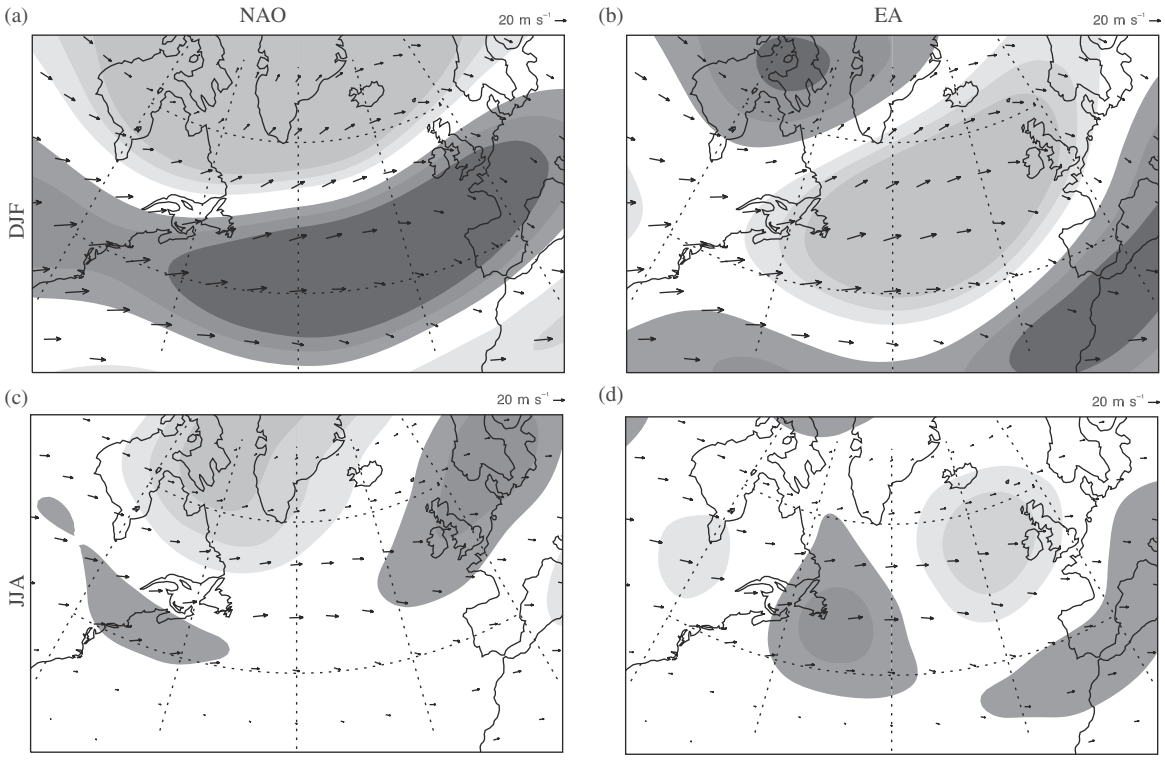

Figure 5. Northern hemisphere teleconnection patterns defined from ERA-Interim data for (a) and (b) winter and (c) and (d) summer. The North Atlantic Oscillation, NAO, pattern ((a) and (c)) and East Atlantic, EA, pattern ((b) and (d)) are shown in their positive phases. The contours represent positive (dark grey) and negative (light grey) geopotential height or pressure anomalies at 250 hPa. The climatological wind vectors are also plotted in each panel.

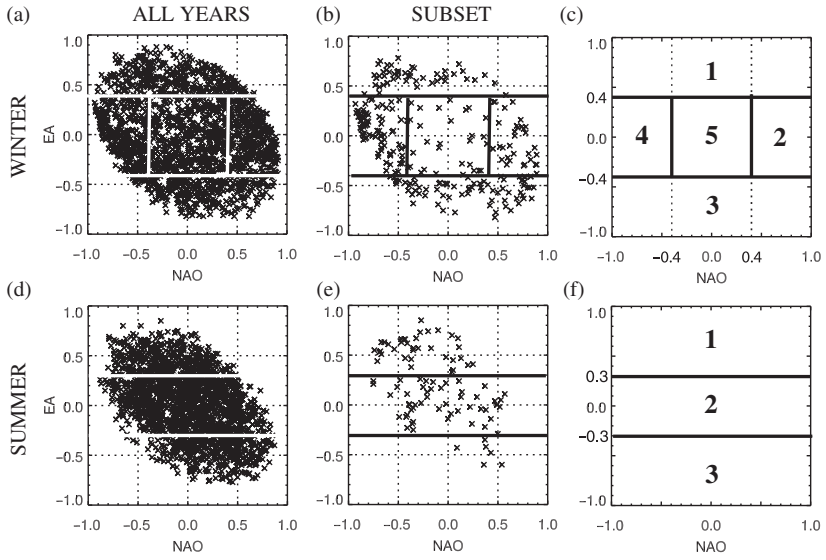

Figure 6. Scatterplot of the projection coefficients obtained by projecting daily Z250 anomalies of ERA-Interim data onto the NAO and EA patterns in winter ((a) and (b)) and summer ((d) and (e)). (a) and (d) show the projection coefficients for all years in ERA-Interim; (b) and (e) show the years for which optimum route data is available for that season (i.e. 2004–2005, 2008–2009 and 2009–2010 for (b) and 2009 for (e)). (c) and (f) show the thresholds used to split the data into five types in winter and three in summer.

The composite Z250 anomaly patterns reflect the NAO and EA patterns that the types were split by. The Z250 anomaly pattern for type W5 does not resemble the EA or NAO as this type has a weak projection onto both patterns of variability. Figure 7 shows that the optimum routes for the different weather types are quite distinct. The individual types are now discussed in turn.

Type W1 is characterized by a strong zonal jet stream and a trough dominating the North Atlantic. This results in the eastbound optimum routes being to the south of the great circle route to benefit from strong tailwinds in the jet stream, and westbound routes to the north of the great circle route to avoid the jet. Types W2 and W3 are characterized by a meridionally tilted jet stream. For type W2, where the jet

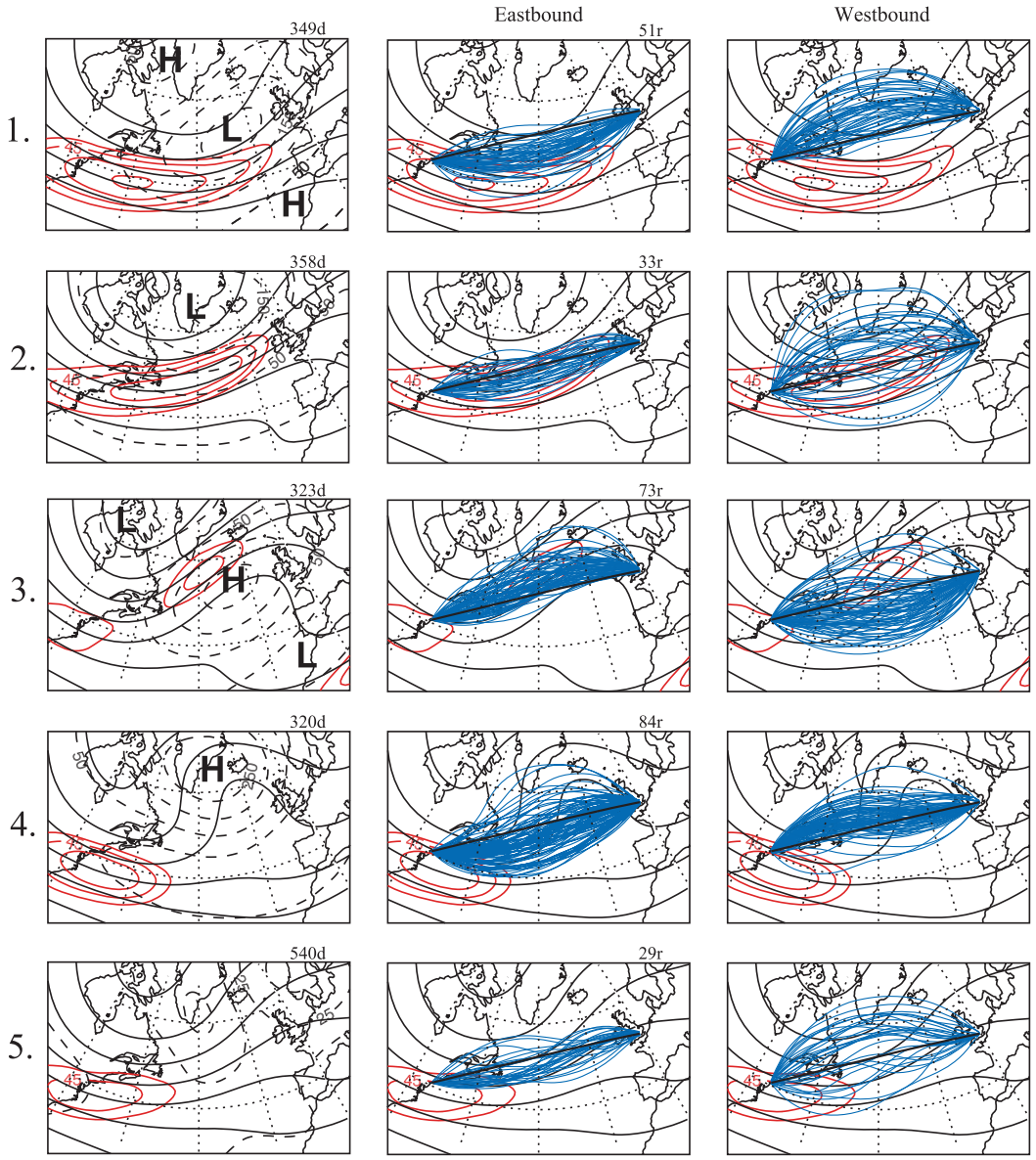

Figure 7. Composites of Z250 (black contours) and v250 above 40 m s^{-1} (red contours with interval 3 m s^{-1}) for each identified weather type in winter are shown in the left, centre and right panels. The composite Z250 anomaly (dashed line) is shown on the left panels, where *H* identifies a high pressure anomaly and *L* a low pressure anomaly. For flights between London and New York the great circle route (thick black line) and optimum routes (blue lines) are shown on the centre (for eastbound) and right (for westbound) panels. The number of days making up the composite, from ERA-Interim (*d*) and number of optimum routes displayed, from the three winters for which we have routes (*r*) are shown at the top right of figure panels (*d* and *r* are the same for both eastbound and westbound cases).

Table 1. Characteristics of North Atlantic weather types for winter (W) and summer (S).

Type	Jet stream		Frequency (days/season)
	Position	Strength	
W1	Zonal	Strong	17
W2	Tilted	Strong	17
W3	Tilted	Weak	15
W4	Confined	Strong	15
W5	Confined	Weak	26
S1	Zonal	Strong	19
S2	Weakly tilted	Weak	55
S3	Strongly tilted	Weak	18

stream lies on an axis with the great circle route, there is little spread in the latitude of the eastbound routes, but much spread in the location of the westbound routes which split between flying north and south of the great circle route. For type W3 the composite jet stream is much weaker and located further north due to ridging over the eastern North Atlantic. The eastbound routes are the most northerly of the five types, and the corresponding westbound routes are mostly southerly. Type W4 is characterized by a strong zonally-oriented jet that is confined near the eastern coast of the USA, with pronounced ridging over the eastern Atlantic extending north as far as Iceland. Due to the lack of consistent strong winds over the North Atlantic in the individual days making up the composite, there is the greatest variation in the location of the eastbound routes. Days

belonging to type W5 have little projection onto either the NAO or EA and the composite jet is weak so the eastbound routes are close to the great circle, and the westbound routes can be either north or south of the great circle route. Type W4 could additionally be split into a type with a confined zonal jet stream with resulting routes south of the great circle route, and a type with a weaker jet stream located further north with resulting routes north of the great circle route. However, it was decided that this extra complexity was not justified.

The frequency of each of the defined weather types can be calculated simply as the average number of days *per* season that each type occurs. The methodology, described in Section 4, was constructed in such a way that it would not identify weather types that occur infrequently. This was necessary as it is only possible to determine the climate impact and perform a full climate-optimization for a limited number of cases, due to the computational cost. Types W1 to W4 occur on average 15–19 days *per* winter (Table 1). Type W5 occurs most frequently (26 days) as expected: for this type the daily anomaly pattern has only a small projection onto the NAO and EA patterns.

5.2. Summer

In summer only three types are defined (labelled as S1 to S3 – see Table 1 and Figure 8), in contrast to five in winter. This is because the teleconnection patterns used are weaker in the summer months, and there is less variation in the jet stream latitude: therefore, increasing the number of types would result in less distinct types. As for the winter types, the Z250 anomaly composites reflect how the data are split into types. The Z250 anomaly patterns look like the positive phase of the EA pattern (type S1) and negative phase (type S3) (Figure 8). Anomaly contours are not plotted for type S2 as this has weak projection onto the EA and the magnitude of the Z250 anomalies is less than 10 m.

Type S1 is characterized by a strong and approximately zonally-oriented jet, although the jet is weaker than in the winter composites. The resulting eastbound optimal routes are south of, but close to, the great circle route, and the westbound routes are generally north of it to avoid the jet stream. Type S3 also has a well-defined but weaker jet that is oriented southwest-northeast across the North Atlantic. The eastbound routes are close to, but to the north of, the great circle routes, and westbound routes are close to the great circle route. Note that only 6 days from summer 2009 fall into this type: therefore, strong conclusions about the location of the optimal routes cannot be drawn from these data. Type S2 has a smaller projection onto the EA, and as for the equivalent winter type, W5, has a less well-defined jet. The eastbound optimum routes are south of the great circle route and the westbound routes are north.

Types S1 and S3 occur with similar frequency (19 and 18 days *per* summer respectively), and type S2 is most common as this type has a weaker projection onto the EA (Table 1). From Figure 8 it is clear that there is less variation in the location of the optimal routes for each weather type in summer than in winter. This is due to the lack of variability in the jet latitude compared to winter, and the reduced strength of the jet stream which makes it harder to separate the daily weather patterns into distinct types that can be characterized by the location and strength of the jet stream.

6. Climate characteristics of defined types

For each type in winter and summer, climate proxies (defined in Section 3.2) are used to give an indication of how the individual climate impacts vary by weather type.

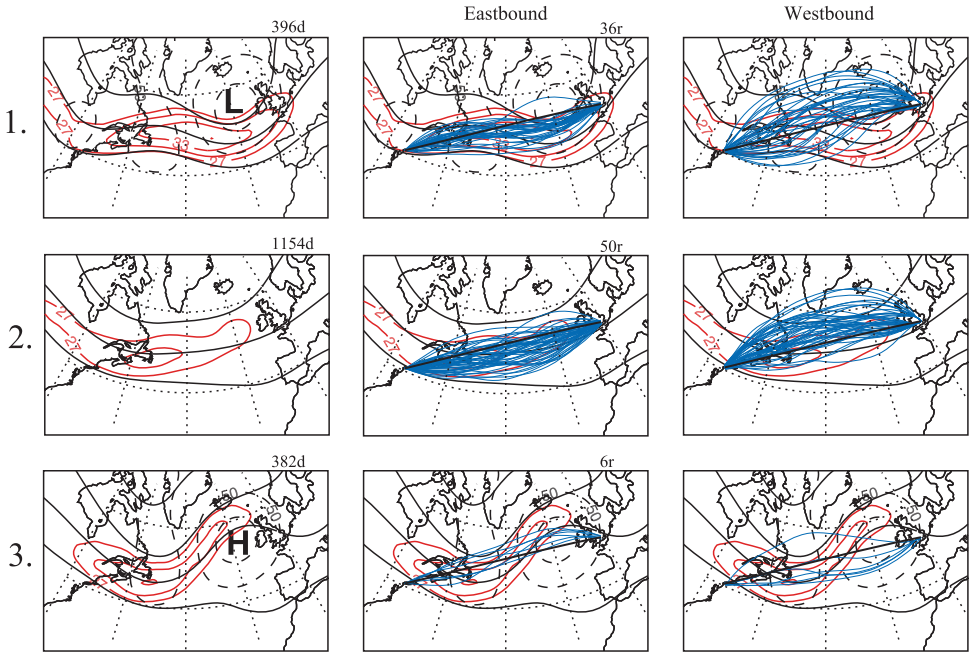

Figure 8. Composites of Z250 (black contours) and v250 above 27 m s^{-1} (red contours with interval 3 m s^{-1}) for each identified weather type in summer are shown in the left, centre and right panels. The composite Z250 anomaly (dashed line) is shown on the left panels, where *H* identifies a high pressure anomaly and *L* a low pressure anomaly. For flights between London and New York the great circle route (thick black line) and optimum routes (blue lines) are shown on the centre (for eastbound) and right (for westbound) panels. The number of days making up the composite, from ERA-Interim (*d*) and number of optimum routes displayed, from the three winters for which we have routes (*r*) are shown at the top right of figure panels (*d* and *r* are the same for both eastbound and westbound cases).

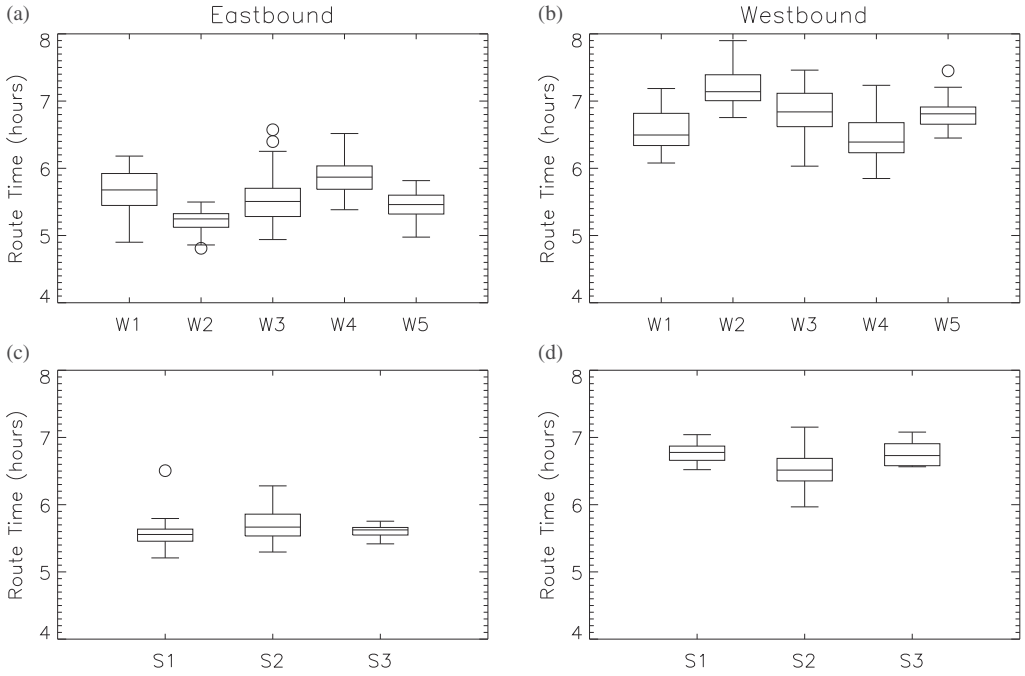

Figure 9. Boxplots of the route times for each type in winter (a), (b) and summer (c), (d). The box encloses the interquartile range (IQR); the whiskers extend to 1.5 × IQR or the data minimum and maximum if there are no data points beyond 1.5 × IQR. Outliers (data points beyond 1.5 × IQR) are marked by circles.

6.1. Winter

The proxy for the CO_2 impact is the route time, illustrated in Figure 9. As eastbound routes generally benefit from strong tailwinds in the jet stream, the route time is shorter and, therefore, eastbound routes almost always have a smaller CO_2 penalty (by typically 20%) than westbound routes (Figure 9(a) and (b)). The actual penalty would also be greater for westbound flights, as due to the longer flights, more fuel must be carried. Of the eastbound routes, type W2 has the smallest CO_2 penalty, as most routes are in the jet and close to the great circle route: however this type has the largest CO_2 penalty for westbound routes. Type W4 has the largest CO_2 penalty for eastbound routes and the smallest for westbound routes.

The proxy for O_3 production is related to the route latitude. It is calculated as the time spent at each latitude band multiplied by a weighting factor (the global-mean radiative forcing that would be produced by flying an aircraft along that latitude band at 250 hPa):

$$M = \frac{\sum_{i=1}^{n} w_i t_i}{n} \qquad (1)$$

where t is the time spent at each latitude band i, w is the latitude weighting and n is the number of latitude bands, equal to 21 for this study. In order to produce a simple proxy a constant fuel burn is employed. In reality, the fuel burn is greater at the start of the flight. The weighting w, shown in Figure 10, is the global-mean O_3 radiative forcing as a function of emission latitude, calculated by adding unit NO_x perturbations to the TRADEOFF 2000 background aircraft emission inventory in the ECHAM climate model (data from Fichter, 2009). NO_x emission perturbations were added at 15, 37, 52 and 74 °N (marked by symbols in Figure 10); to obtain intermediate values of the weighting function, the radiative forcing values were linearly interpolated to the required latitude. Separate weighting functions are used for winter and summer. There are two contributing effects to the O_3 proxy: longer routes will produce more NO_x and therefore lead to greater O_3 production than shorter routes at the same latitude, and southerly routes would lead to more O_3 production than northerly routes due to the more efficient photochemical O_3 production at lower latitudes. Table 2 shows the O_3 proxy (the absolute value is arbitrary as it depends on the assumed NO_x emission perturbation in the climate model, it is the relative size that is important). For the winter routes, the largest impact from O_3 is type W3 westbound, as the routes spend a long time at the southerly latitudes. In general westbound routes will lead to greater O_3 production than eastbound routes as they are longer (Figure 9). However,

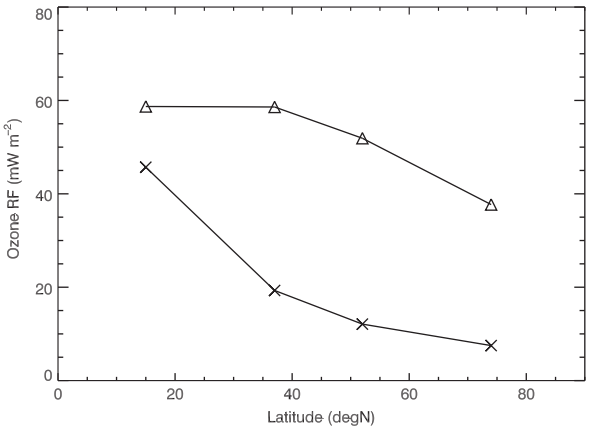

Figure 10. Global-mean O^3 radiative forcing from aviation NO_x emissions at 250 hPa as a function of emission latitude for winter (crosses) and summer (triangles). The forcing is calculated assuming a constant emission of NO_x equivalent to 1 Tg (N) *per* year at each latitude. Data from Fichter (2009).

Table 2. Climate-Impact proxies for aircraft flying on optimum routes through North Atlantic weather types in winter (W) and summer (S).

Type	O_3 proxy ± std dev(mW m^{-2} s)		t_{strat} ± std dev (mins)		$P(d < 100$ km), $P(d < 500$ km)	
	E-bound	W-bound	E-bound	W-bound	E-bound	W-bound
W1	233 ± 19	231 ± 11	263 ± 54	324 ± 66	0.49, 0.86	0.63, 0.86
W2	202 ± 12	261 ± 34	167 ± 52	279 ± 125	0.21, 0.55	0.36, 0.85
W3	200 ± 11	280 ± 33	154 ± 49	159 ± 94	0.25, 0.66	0.38, 0.77
W4	233 ± 22	237 ± 17	233 ± 56	255 ± 62	0.48, 0.87	0.48, 0.93
W5	211 ± 11	252 ± 30	178 ± 54	257 ± 62	0.20, 0.72	0.34, 0.86
S1	847 ± 31	994 ± 45	144 ± 31	223 ± 75	0.25, 0.78	0.28, 0.83
S2	868 ± 39	957 ± 35	146 ± 47	227 ± 82	0.26, 0.80	0.30, 0.70
S3	834 ± 11	1030 ± 18	102 ± 32	96 ± 83	0.17, 0.50	0.17, 0.83

For the O_3 and t_{strat} proxies the mean value and standard deviation are shown. For contrails the probability P of contrail distances being less than 100 km or 500 km is shown for both eastbound and westbound flights.

the value given by the proxy is similar for types W1 and W4: eastbound routes in type W1 spend less time at southerly latitudes and the westbound routes, although more northerly, are much longer than the eastbound routes (Figure 9).

The climate impact for water vapour, and to some extent NO_x, is increased if the water vapour is emitted into the stratosphere. Therefore, the proxy for the climate impact of water vapour emissions is the total route time that the aircraft spends in the stratosphere, t_{strat}. Here, following Wilcox *et al.* (2011), the tropopause is defined by the 2 PVU surface. There are large gradients in the height of this surface around weather systems, where there may be tropopause folds, and also crossing the jet stream where there is a sharp increase in tropopause height from the polar to equatorward side. Although the standard deviations are quite large, types W1 and W4 (eastbound) have the greatest times (t_{strat}) in the stratosphere, as the routes are north of the jet (Table 2). The weather situation in Figure 4(a), where the route was almost entirely in the stratosphere belongs to type W1. Type W3 has the smallest time in the stratosphere; Figure 4(b) belongs to Type W3. Correspondingly for westbound flights, type W1 spends the most time, on average 324 min (0.82 of the total route time), in the stratosphere as the routes are far north of the jet, flying through a trough. Type W3 spends the least time in the stratosphere as the routes are south of the jet in a situation of weak ridging.

Persistent contrail-supporting areas are defined as regions where the relative humidity is supersaturated with respect to ice and the temperature is below 233 K. As noted above, this definition does not preclude contrails in the stratosphere. Figure 11 shows the frequency distribution of the total distance over which an aircraft would produce a persistent contrail for winter types 1–4; the distribution for type 5 is similar to type 2 and is not shown. For all types the distributions have a peak at 0–100 km: however the shape of the distributions differs by type. It is clear from the distributions, that using the mean and standard deviation of the distance contrailing as a proxy for the climate impact from contrails is not an effective discriminator between types, as the mean values (not shown) are inflated by large rare values, and the distributions are non-Gaussian and highly skewed towards zero contrails. Therefore the probability that the contrail distance is less than 100 km ($P < 100$ km) and 500 km ($P < 500$ km) is used as our climate impact proxy for contrails (Table 2). The total distance over which an aircraft would produce a persistent contrail is largest for routes which spend the most time in the troposphere, as this increases the likelihood of flying through a super-saturated region. Thus, the probability of the total contrail distance being less than 500 km is smallest for type W2 eastbound and type W3 westbound (Table 2). Types 1 and 4 have the greatest probability of producing less contrails, both for eastbound and westbound routes. On rare occasions, the total distance for which persistent contrails are predicted to occur exceeds 20% of the route distance. The size of the contrail distance is sensitive to the relative humidity threshold used to define a persistent contrail-supporting area: using a threshold of 95% instead of 100% the mean contrail distance is tripled, and using a threshold of 90% the contrail distances are quadrupled (not shown). This is true for all types, however the frequency distributions are similar and therefore the sensitivity of the contrail distance to the relative humidity threshold used does not affect the conclusions drawn.

In summary, the climate impact of CO_2, NO_x, and H_2O emissions, and of contrails, varies according to the weather type. It is also interesting to note that regardless of weather type, the climate impact of westbound routes is always greater than that of eastbound routes.

6.2. Summer

The CO_2 impact for the summer weather types is assessed using the route time proxy (Figure 9(c) and (d)). The mean route times are similar, suggesting that the CO_2 impact would be similar for each route. This variation, of less than 20 min in the mean route times for the summer types, is half the range of over 40 min for the winter types. However, the route time for type S2 has a range of over one hour, double the range for types S1 and S3. This range is likely to be due to the variation in the strength of the jet stream and results in a larger spread for the CO_2 impact for this type.

O_3 impact is calculated using Equation (1), with the weighting function for summer based on results from Fichter (2009) (Figure 10). In summer this weighting function (O_3 radiative forcing) has a larger gradient over the range of latitudes 40–70 °N, where the majority of the trans-Atlantic traffic is found, than in winter. Types S1 and S2 would lead to a slightly higher climate impact from O_3 than type S3 for eastbound routes and vice-versa for westbound routes (Table 2). The O_3 production is much greater in summer due to the increased availability of sunlight, which is necessary to form O_3. Correspondingly, the O_3 proxy for the types in summer is approximately four times larger than the O_3 proxy for the winter routes (Table 2), although the net climate effect of the NO_x emissions would also need to take into account the accompanying decrease in methane (see Section 3.2).

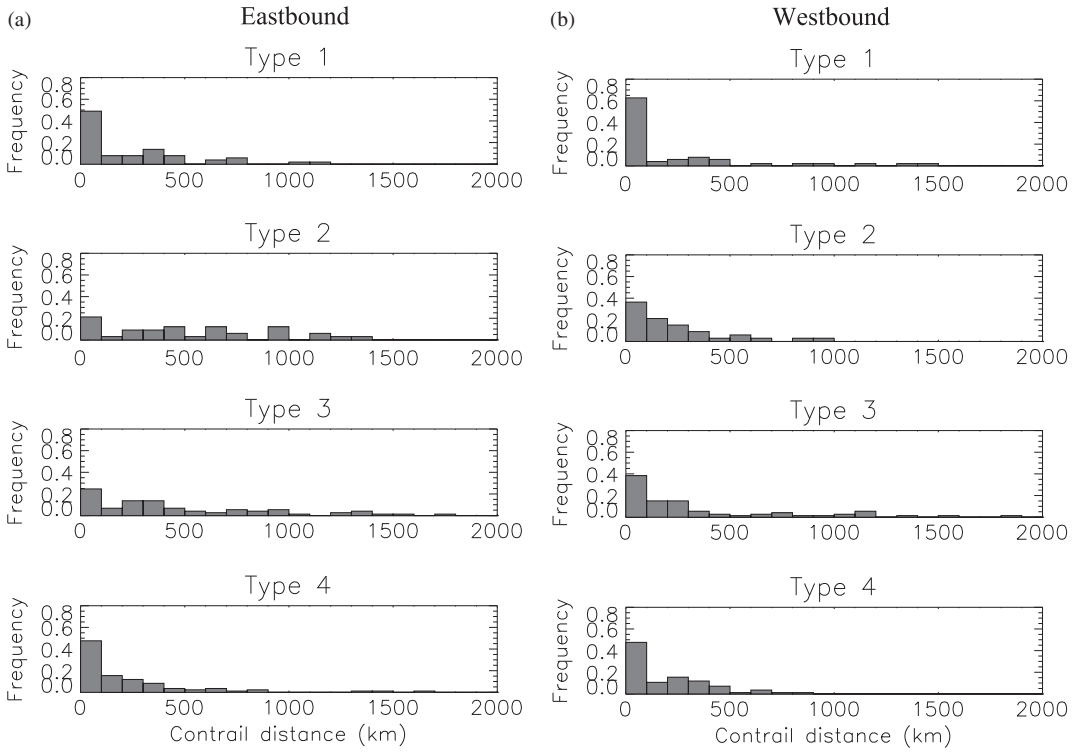

Figure 11. Relative frequency distribution of contrail distance by type in winter for (a) eastbound and (b) westbound routes. Frequencies sum to 1.

The climate impact of water vapour depends on the route time in the stratosphere. Type S3 has the smallest time in the stratosphere, at 102 min for eastbound routes and 96 min for westbound routes (Table 2). This is because for this type the optimum routes spend most time south of the jet stream where there is pronounced ridging in the eastern North Atlantic which would be associated with higher tropopause heights. Types S1 and S2 spend more time in the jet stream or north of the jet stream where the tropopause is lower and, therefore, the route time in the stratosphere is higher for these types, particularly for westbound routes. As the tropopause is generally higher in summer it might be expected that the time spent in the stratosphere would be lower than for the winter routes. This is true for the eastbound routes, where t_{strat} is lower than the winter values. This is not the case for westbound types S1 and S2 as these are north of the jet stream, and the times are within the range found for westbound flights in winter (Table 2).

The probability of the total contrail distance being less than 500 km is smallest for type S3 eastbound, where the aircraft spends the smallest amount of time in the stratosphere (Table 2). With the exception of type S3 eastbound, there is little variation between types in the distribution of total contrail distance. It is also interesting to note that, for a fixed altitude of 250 hPa, the mean contrail distances, which correspond to approximately 0.1 of the total route distance (not shown), are similar in summer and winter, even though in winter the routes would spend more time in the stratosphere due to the lower tropopause.

In summary, the climate impact of westbound routes is always greater than for eastbound routes, as was seen for the winter weather types. The variation in climate impact between types is smaller in summer than winter. The climate impact of NO_x is clearly greater in summer, whereas the impacts of water vapour and contrails are smaller.

7. Conclusions

The climate impact of a single flight varies according to the emission location and ambient atmospheric conditions. It should, therefore, be possible to optimize a route so that the emissions have the minimum climate impact. To facilitate the minimization for trans-Atlantic flights, a set of relevant weather types, commonly occurring weather patterns, are defined for the North Atlantic region, for both summer and winter. Daily patterns are classified into types according to the similarity of the daily geopotential height anomaly at flight level (250 hPa) to the NAO or EA teleconnection patterns. This results in five types being defined for winter and three for summer. The types can be characterized by the strength and location of the jet stream at 250 hPa. The optimal routes, specifically the New York to London route, have different characteristics for each type.

In order to assess whether the different aviation climate impacts vary amongst the different weather types, proxies for the climate impact are identified. These are highly simplified in order to be computed without detailed knowledge of aircraft or engine type, fuel burn or the fate of the aircraft emissions (therefore the results are independent of aircraft and engine type) and are used only to illustrate that different climate impacts might be expected by flying through different weather types. The climate impact of CO_2 is independent of the location of its emission and, therefore, only the amount of CO_2 emitted and not its location are of concern. Assuming constant flight level and fuel burn the amount of CO_2 emitted is related to the air-distance travelled. As a constant airspeed was also used, the simple proxy for the climate impact of CO_2 is the route time, which varies by over an hour during winter. The climate impact of the effect of aviation NO_x emissions on O_3 depends on the latitude and altitude of the emission: as a constant altitude is considered the proxy for the O_3 impact is a function of the emission latitude and time spent at that latitude. The range

in route latitudes is determined by the jet latitude: the route latitudes vary between 40 and 70 °N. The proxy for the water vapour impact is the route time in the stratosphere. This is on average 0.6 of the total route time in winter, and 0.4–0.5 in summer depending on the direction of the route. The distance in which contrails may be produced is smaller but comparable for summer and winter, and on 12% of winter days stratospheric contrails are possible.

The climate impact varies both by season, type and direction of flight, as eastbound and westbound flights rarely fly the same route through a weather pattern. The main points are that the climate impact of westbound flights is greater than that of eastbound flights. In winter there is a larger impact from contrails and water vapour and smaller impact from NO_x, compared to summer. The variation between types is smaller in summer than winter. The CO_2 impact of eastbound flights is smallest for types which have a strong jet that is tilted northeastwards towards the UK, and largest for types that have weak tailwinds. The ozone impact is largest for flights which take southerly routes with weak tailwinds (i.e. spend more time at southerly latitudes), or long routes. This means that, in general, westbound routes will lead to greater O_3 production than eastbound routes as they are longer. The water vapour impact is largest for types where the optimal routes lie north of the jet stream, due to the decrease in tropopause height from the south to the north of the jet stream. Lastly, total contrail distance size distribution varies according to type, with a peak between 0 and 100 km: large distances of over 1000 km are rare. The mean impact of contrails varies between 5 and 10% of the route distance. However, it is much more variable amongst routes for the same weather type (than between the weather types) and hence is less clearly related to the individual weather type. This is likely to be due to the variety of formation processes for ice-supersaturated regions where contrails form, such as uplift of air by gravity waves or warm conveyor belts of mid-latitude weather systems (Spichtinger *et al*., 2005a,b) which occur for all types.

The weather types are reasonably successful at discriminating cases with long flight times (and therefore high CO_2 emissions) relative to cases with short flight times. It could be judged that the types are less successful at discriminating between cases of high and low ozone impact, or water vapour impact, given that the mean values of the proxies for each type are often within one standard deviation of each other. However, it is argued that this is difficult to ascertain directly, as it is not known if it is really possible to discriminate between these cases. In this paper the effect of flying at different cruise altitudes is deliberately neglected in the calculation of the proxies. Higher cruise altitudes lead to the aircraft spending more time in the stratosphere, which increases the lifetime of water vapour and NO_x and, therefore, increases the impact from O_3. However, without the use of a detailed fuel burn model, it is difficult to compare the values of the proxies used here at different altitudes. For example, in the case of using the route time as a direct proxy for CO_2 emissions, the amount of fuel burned, and therefore CO_2 emitted, varies according to the altitude of the aircraft (as aircraft engines are most efficient at a particular altitude).

In order to compute the climate proxies, and in the calculation of the time-optimal routes some assumptions which simplify the behaviour of the aircraft during flight have been made. It is assumed that the aircraft flies at a constant altitude and with constant airspeed, and have placed no restrictions on the location of the route. In reality, an aircraft may vary its airspeed according to the strength of the winds it is flying through, so that the balance between time and fuel use is most economical. The optimal cruise altitude of an aircraft also increases during the flight as an aircraft burns off fuel and becomes lighter. However, air traffic over the North Atlantic is heavily constrained due to the volume of air traffic and lack of radar coverage, which may require an aircraft to fly at a set altitude and speed as it crosses the North Atlantic (or at least it limits the number of altitude changes). It also may not be possible for an aircraft to fly a time-optimal route due to air traffic or operating constraints. Despite their limitations, the assumptions made here are sufficient for the determination of characteristic weather types and the likely relation between the winds associated with these types and possible aircraft trajectories through them. The detailed climate impact assessments will be carried out for the climate optimization of the routes in the REACT4C project, which will take into account air traffic and operating constraints on the aircraft routings and also allow the different aviation climate impacts to be placed on a common scale.

Acknowledgements

The authors would like to acknowledge Lauren Reid and Andrew Mirza at the Met Office who provided the optimum route data. Emily Martin at NATS kindly provided North Atlantic track data, and assisted in locating the named waypoints in the data. The ozone forcings were calculated within the PhD thesis of the last author Christine Frömming, which was published under her maiden name Christine Fichter. Volker Grewe provided helpful comments on an earlier draft. Very helpful comments from referees are also acknowledged. This work forms part of the REACT4C project, funded under the EU Seventh Framework Programme, grant ACP8-GA-2009-233772.

References

Barnston AG, Livezey RE. 1987. Classification, seasonality and persistence of low-frequency atmospheric circulation patterns. *Mon. Weather Rev.* **115**: 1083–1126.

Dee DP, Uppala SM, Simmons AJ, Berrisford P, Poli P, Kobayashi S, Andrae U, Balmaseda MA, Balsamo G, Bauer P, Bechtold P, Beljaars ACM, van de Berg L, Bidlot J, Bormann N, Delsol C, Dragani R, Fuentes M, Geer AJ, Haimberger L, Healy SB, Hersbach H, Hólm EV, Isaksen L, Kållberg P, Köhler M, Matricardi M, McNally AP, Monge-Sanz BM, Morcrette J-J, Park B-K, Peubey C, de Rosnay P, Tavolato C, Thépaut J-N, Vitart F. 2011. The ERA-Interim reanalysis: configuration and performance of the data assimilation system. *Q. J. R. Meteorol. Soc.* **137**: 553–597.

Fichter C. 2009. Climate impact of air traffic emissions and dependency of the emission location and altitude. *DLR Forschungsberichte* **22**: ISSN: 1434–8454. 152 pp.

Forster C, Stohl A, James P, Thouret V. 2003. The residence times of aircraft emissions in the stratosphere using a mean emission inventory and emissions along actual flight tracks. *J. Geophys. Res.* **108**(D12): 8524.

Fuglestvedt JS, Shine KP, Cook J, Berntsen T, Lee DS, Stenke A, Skeie RB, Velders GJM, Waitz IA. 2010. Assessment of transport impacts on climate and ozone: metrics. *Atmos. Environ.* **44**: 4648–4677.

Gettelman A. 1998. The evolution of aircraft emissions in the stratosphere. *Geophys. Res. Lett.* **25**(12): 2129–2132.

Gierens KM, Schumann U, Helten M, Smit H, Marenco A. 1999. A distribution law for relative humidity in the upper troposphere and lower stratosphere derived from three years of MOZAIC measurements. *Ann. Geophys.* **17**: 1218–1226.

Grewe V, Stenke A. 2008. AirClim: an efficient tool for climate evaluation of aircraft technology. *Atmos. Chem. Phys.* **8**: 4621–4639.

ICAO. 2008. *North Atlantic Minimum Navigation Performance Specification Airspace Operations Manual*. International Civil Aviation Organisation: Montréal, Canada. http://www.ibac.org/Files/CNSA TM/Library/MNPSA_2008.pdf (accessed 8 December 2011).

Lee DS, Fahey DW, Forster PM, Newton PJ, Wit RCN, Lim LL, Owen B, Sausen R. 2009. Aviation and global climate change in the 21st century. *Atmos. Environ.* **43**: 3520–3537.

Lee DS, Pitari G, Grewe V, Gierens K, Penner JE, Petzold A, Prather MJ, Schumann U, Bais A, Berntsen T, Iachetti D, Lim LL, Sausen R. 2010. Transport impacts on atmosphere and climate: aviation. *Atmos. Environ.* **44**: 4678–4734.

Lunnon RW. 1992. Optimization of time saving in navigation through an area of variable flow. *J. Navig.* **45**: 384–399.

Michelangeli P-A, Vautard R, Legras B. 1995. Weather regimes: recurrence and quasi-stationarity. *J. Atmos. Sci.* **52**: 1237–1256.

NATS. 2010. *NATS and the Environment, Acting Responsibly 2010*. National Air Traffic Services report. National Air Traffic Services: Fareham, UK. http://www.nats.co.uk/wp-content/uploads/2010/09/Acting-Responsibly-ATM-CO2-Annual-Report-2010-FINAL-HQ.pdf (accessed 8 December 2011).

Rädel G, Shine KP. 2010. Validating ECMWF forecasts for the occurrence of ice super saturation using visual observations of persistent contrails and radiosonde measurements over England. *Q. J. R. Meteorol. Soc.* **136**: 1723–1732.

Ren L, Reynolds TG, Clarke J-PB, Hooper DA, Parton GA, Dore AJ. 2010. Meteorological influences on the design of advanced aircraft approach procedures for reduced environmental impact. *Meteorol. Appl.* **18**: 40–59.

Schumann U. 1996. On conditions of contrail formation from aircraft exhausts. *Meteorol. Z.* **5**: 4–23.

Spichtinger P, Gierens K, Read W. 2003. The global distribution of ice-supersaturated regions as seen by the microwave limb sounder. *Q. J. R. Meteorol. Soc.* **129**: 3391–3410.

Spichtinger P, Gierens K, Wernli H. 2005a. A case study on the formation and evolution of ice supersaturation in the vicinity of a warm conveyor belt's outflow region. *Atmos. Chem. Phys.* **5**: 973–987.

Spichtinger P, Gierens K, Dörnbrack A. 2005b. Formation of ice supersaturation by mesoscale gravity waves. *Atmos. Chem. Phys.* **5**: 1243–1255.

Tompkins AM, Gierens K, Rädel G. 2007. Ice supersaturation in the {ECMWF} integrated forecast system. *Q. J. R. Meteorol. Soc.* **133**: 53–63.

Vautard R. 1990. Multiple weather regimes over the North Atlantic: analysis of precursors and successors. *Mon. Weather Rev.* **118**: 2056–2081.

Wilcox LJ, Hoskins BJ, Shine KP. 2011. A global blended tropopause based on ERA data. Part 1: Climatology. *Q. J. R. Meteorol. Soc.* DOI: 10.1002/qj.951.

Wilkerson JT, Jacobson MZ, Malwitz A, Balasubramanian S, Wayson R, Fleming G, Naiman AD, Lele SK. 2010. Analysis of emission data from global commercial aviation: 2004 and 2006. *Atmos. Chem. Phys.* **10**: 6391–6408.

Woollings T, Hannachi A, Hoskins B. 2010. Variability of the North Atlantic eddy-driven jet stream. *Q. J. R. Meteorol. Soc.* **136**: 856–868.

